韓國港灣學會 第11卷 第2號, pp.215~230. 1997.

論 文

Plume Rise and Initial Dilution Determination Reflecting the Density Profile over Entire Water Column

S. J. Kwon · J. W. Lee***

해수 전체 컬럼에서 밀도 분포를 반영한 플룸 상승과 초기 희석도 결정

권 석 재 · 이 중 우

Key Words : Ocean Outfall(해양 배출구), Plume Rise(플룸 상승), Initial Dilution(초기 희석), Surfacing Frequency(표면상승 빈도), CTD data(전도, 온도, 수심 자료), Density Stratification(밀도 성층화), Density Gradient(밀도 경사), Diffuser (확산기).

Abstract

A number of ocean outfalls are located around coastal area over the United States and discharge primary treated effluent into deep water for efficient wastewater treatment. Two of them, the Sand Island and Honouliuli municipal wastewater outfalls, are located on the south coast of Oahu. There have been growing interests about the plume dynamics around the ocean outfalls since plume discharged from the multiport diffuser may have significant impacts on coastal communities and immediate consequence on public health.

Among the studies of plume dynamics performed in the vicinity of both outfalls, Project MB-4 in the Mamala Bay Study recently made with the funding in the $ 9 million amount statistically dealt with the near-field behavior of the plumes at the Sand Island and Honouliuli outfalls. However, Project MB-4 predicted much higher surfacing frequency than the realistic value obtained by model studies by Oceanit Laboratories, Inc.. It is suggested that improvements should be made in the application of the plume model to more simulate the actual discharge characteristics and ocean conditions.

In this study, it has been recommended that input parameters in plume models reflect

* 정회원, Dept. of Ocean Engineering, University of Hawaii
** 정회원, 한국해양대학교 토목 공학과 교수

realistic density profile over the entire water column since, in the previous Mamala Bay Study, the density profiles were measured at 5m depth increments extending from 13 to 63 m depth (the density profile on the upper portion of water column was not included, Roberts 1995). It is proved that the density stratification is the important parameter for the submergence of the plume. In this study, as one of the important parameters, plume rise and initial dilution reflecting the density profile over the entire water column have been taken into account for more reliable plume behavior description.

1. Introduction

The study sites are the Sand Island and Honouliuli municipal wastewater outfalls located on the south coast of Oahu as shown in Fig. 1. The distribution of the diffusers and the monitoring stations where density profiles were measured along entire depth are also shown in Fig. 1. One of the studies of plume dynamics carried out around the both outfalls, Project MB-4 in the Mamala Bay Study made with funding in the amount of $9 million, contains a section dealing with model calculations of the plume rise and initial dilution of the Sand Island and Honouliuli wastewater discharges. In this Project, the RSB model was chosen for the calculation of the near field plume behavior based on bottom currents measured in Project MB-6, treatment plant flows, and density profiles measured simultaneously on a halfhour time interval (Roberts, 1995). In the case of the Sand Island Outfall, these model calculations indicate a more frequent surfacing frequency of 22.4 %. However, this surfacing has not been noticed in the ocean, and the frequency of surfacing obtained by model studies by Oceanit Laboratories, Inc. were approximately 2 %.

In project MB-6, density profiles were measured as 11 thermistors on each chain at 5 m depth increments extended from 13 to 63 m depth at the Sand Island Outfall and 15 to 65 m depth at the Honouliuli outfall. In other words, the density profiles entered as input in the Mamala Bay Study did not cover the upper portion of the water column. However, in this study, density profiles measured in 1 m depth

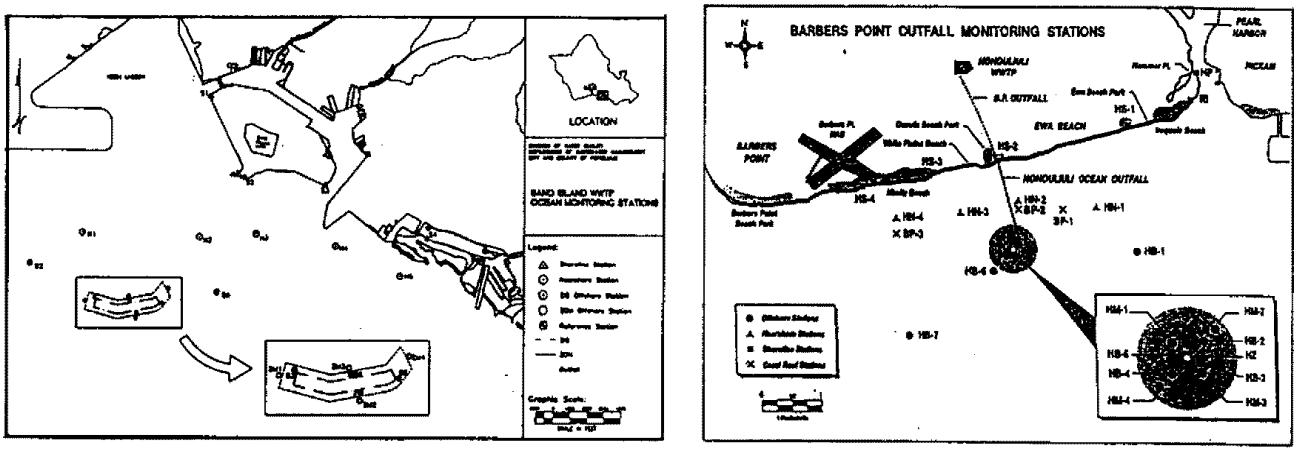

Fig. 1 Plan View of the Sand Island and Honouliuli Ocean Monitoring Stations (City and County of Honolulu)

increments over entire water column have been obtained from the City and County of Honolulu and used for more reliable and justifiable plume behavior description. The UM and RSB models are reliable and recent models which will be used herein for the prediction of wastefield behavior at both outfalls since both models support each other, but are certainly identical. It is expected that this study provide a standard technique to evaluate future data and the plumes of other outfalls.

2. Chosen Plume Models

2.1 Review of the RSB and UM Models

The procedure to estimate the initial dilution and describe the zone of initial dilution near the diffuser is specified in US Environmental Protection Agency (EPA) regulations. The RSB (Roberts-Snyder-Baumgartner) model approved by EPA is a more suitable model than any other previous model since this model is based on the experimental studies of multiport diffusers in density-stratified currents. Significantly, the model also takes into account the merging of plumes from both sides of the diffuser and re-entrainment and additional mixing in the spreading layer. The surfacing plume generated by stratified or unstratified density conditions can be predicted by the RSB model thereby overcoming the deficiency of the ULINE model. However, it should also be noted that RSB is based on an uniform current, linear density stratification, and straight line diffusers (Roberts, 1995).

The latest model approved by the EPA is the UM (Updated Merge) model developed for marine applications by Teeter and Baumgartner (1979). Since the UMERGE model has been generalized and improved, the UM model includes the improvements. The prominent features in the UM model includes Lagrangian formulation and Projected Area Entrainment (PAE) hypothesis which is also supported by the experimental data on which the RSB model is based. The UM model is suitable for a similar range of conditions for single port as well as multiport discharges, but only for the ports along one side. The UM model can handle vertical nonuniformities in current speed and direction which are not applicable in the RSB model. Since the UM model is not constrained by the Boussinesq approximations, this model can handle negatively buoyant flows for dense discharges. However, the limitations are that the UM is less useful for the cases of currents parallel to the diffuser, for shallow water, and for plumes discharging to very cold or fresh water (Baumgartner, 1994).

As described above, the UM and the RSB models are reliable and recent models which will be used herein for the prediction of wastefield behavior at both outfalls. It is difficult to determine at the outset which model is more suitable for these outfalls since both models support each other, but are certainly not identical. The results predicted by the RSB and UM models will be compared for a range of plume behavior.

2.2 RSB Mathematical Description

Currents and density stratification are the oceanic characteristics which significantly affect initial mixing. The discharge from a diffuser can be described by the volumetric flux, q, momentum, m, and buoyancy, b, per unit diffuser length:

$$q=\frac{Q}{L} \quad m=u_j q \quad b=g'_0 q \qquad \cdots\cdots (1)$$

where Q is the total discharge, L is the diffuser length, $g'_0 = g(\rho_a - \rho_0)/\rho_a$ is the reduced gravitational acceleration due to gravity, ρ_a is ambient density, and ρ_a is the effluent density. When the stratification is linearized over the height of rise, it can be described by the buoyancy frequency N as

$$N = \pm\left(\frac{g|d\rho|}{\rho_a\, dz}\right)^{0.5} \quad \cdots\cdots (2)$$

where ρ_a is the density of ambient water at height z above the diffuser, and g is the acceleration due to gravity.

The three length scales can be expressed in terms of source volume flux, momentum, buoyancy, and buoyancy frequency as

$$l_q = \frac{q^2}{m} \quad l_b = \frac{b^{1/3}}{N} \quad l_m = \frac{m}{b^{2/3}} \quad \cdots\cdots (3)$$

The current flows with a speed u at an angle Θ to the diffuser axis. The geometrical characteristic variables involved in this process are given by

$$z_e,\ h_e,\ z_m = f(q,\ b,\ m,\ s,\ u,\ N,\ \Theta) \quad \cdots\cdots (4)$$

where s is the port spacing. Three important dimensionless dynamical parameters which characterize the flow are based on the total fluxes. A useful form for the functional relationship, through dimensional analysis, is given by

$$\frac{z_e}{l_b},\ \frac{h_e}{l_b},\ \frac{z_m}{l_b} = f\left(\frac{l_m}{l_b},\ \frac{s}{l_b},\ F,\ \Theta\right) \quad \cdots\cdots (5)$$

where z_e is the height to the top of the established wastefield, h_e is the thickness of the established wastefield, two length scale ratios, l_m/l_b and s/l_b, indicate the significance of source momentum flux and port spacing (Wright et al., 1982), and $F = u^3/b$ is a dynamic variable similar to the Froude number. It should be noted that the two length scales involve the jet exit velocity, port spacing, port diameter, effluent density, and ambient stratification. The effect of the volume flux q is slight except in regions very close to the ports since l_q/l_b is generally much less than one. The corresponding normalized expression for dilution can then be described in dimensionless form as:

$$\frac{S_m qN}{b^{2/3}} = f\left(\frac{l_m}{l_b},\ \frac{s}{l_b},\ F,\ \Theta\right) \quad \cdots\cdots (6)$$

where the minimum initial dilution, S_m, is the smallest value at the established value (Baumgartner, Frick, and Roberts, 1994).

In the hydraulic model tests (Roberts, 1989), the ranges of experiments for actual operating conditions were chosen as $0.078 < l_m/l_b < 0.5$ and $0.31 < s/l_b < 1.92$ while the ranges were limited to $l_m/l_b < 0.2$ and $s/l_b < 0.3$ for a line plume. The effect of source momentum flux is neglected since the individual plumes are rapidly merged. Therefore, it should be noticed that the ranges may be considered as $l_m/l_b < 0.5$ and $s/l_b < 1.92$ for many ocean outfalls operated in the regime where momentum flux is neglected.

The importance of the current speed relative to the buoyancy flux of the source can be described by the dynamic variable, F. Corresponding to the different current speeds, the tests were run for a range of the F of 0 to 100. Larger values of F gave higher dilution due to increased current speed which causes the plumes to be rapidly swept downstream. There is no effect of currents on dilution when $F < 0.1$.

The direction of the current relative to the diffuser also affects plume behavior. Tests were run for cases of (1) the diffuser perpendicular ($\Theta = 90°$), (2) diagonal ($\Theta = 45°$), and (3) parallel

(Θ=0°) to the current. The highest initial dilution and lowest rise height generally result from the diffuser being perpendicular to the current.

2.3 UM Mathematical Description

The projected area entrainment hypothesis can be expressed in terms of vectors as

$$\frac{dm}{dt} = -\rho_a \overline{A_p} \cdot \overline{U} \quad \cdots\cdots (7)$$

where dm is the incremental amount of mass entrained in the time increment dt, ρ_a is ambient density, $\overline{A_p}$ is the projected area in a vertical plane containing the current vector and points upstream out of element, $\overline{U}$ is the average velocity of the ambient flow normal to the projected area. The number of the increments depends on how much the local current velocity differs from the element velocity.

The complete entrainment equation can be expressed as a sum of the forced and Taylor induced entrainment terms

$$\frac{dm}{dt} = -\rho \overline{A_p} \cdot \overline{U} + \rho A_T \cdot v_T \quad \cdots\cdots (8)$$

where A_T is the plume element area contacting with the ambient fluid and v_T is Taylor aspiration speed.

The Taylor aspiration area without merging, dynamic collapse, and element overlap can be expressed simply by

$$A_T = 2\pi bh \quad \cdots\cdots (9)$$

where b is the element radius. However, the UM does not include the effects of dynamic collapse.

The ambient current velocity vector can be stated as the sum of components in terms of the local coordinate system

$$\overline{U} = u_1 \bar{e}_1 + u_2 \bar{e}_2 + u_3 \bar{e}_3 \quad \cdots\cdots (10)$$

where $\bar{e}_1$, $\bar{e}_2$, and $\bar{e}_3$ are the unit vectors in the direction of trajectory, the horizontal normal to the trajectory, and in a vertical plane.

The projected area associated with u_1, A_1, is simply the area which wraps the plume element side and is given as

$$A_1 = \pi b \Delta b \quad \cdots\cdots (11)$$

where Δb is the difference between the radius of the trailing and leading plume element faces that can be expressed as

$$\Delta b = \frac{\partial b}{\partial s} h \quad \cdots\cdots (12)$$

where s is the distance along the centerline. The cylinder projected area is

$$A_{cyl} = 2bh \quad \cdots\cdots (13)$$

When the face of the element normal to s is deformed by strong trajectory curvature, the projected area can be given by

$$A_{cur} = -\frac{\pi b^2}{2} \frac{\partial \theta}{\partial s} h \quad \cdots\cdots (14)$$

where θ is the elevation angle of s. The positive or negative value of this area depends on the sign of $\partial\theta/\partial s$ determined by reference to successive value of $\overline{U}$.

Conservation of momentum is expressed

$$\frac{dm\overline{V}}{dt} = \overline{U}\frac{dm}{dt} - m\frac{(\rho_a - \rho)}{\rho}\overline{g} \quad \cdots\cdots (15)$$

where $\overline{V}$ is plume element velocity vector, m is the plume element mass ($m = \rho\pi b^2 h$), $\overline{g}$ is the gravity vector, and ρ_a and ρ are the ambient and average element densities. In other words, the change of momentum in the element results from the amount of momentum generated by the

entrained mass (dm) and the vertical momentum change generated by the buoyant force. It is assumed that there are no shears which can generate drag effects, and that the bottom is flat. When a plume reaches the water surface, the predicted dilution is reduced by 10 % (Muellenhoff et al 1985). It is assumed that radiation, conduction, and diffusion are small. The conservation of energy and salinity can also be derived in a similar way.

The boundary conditions include the initial plume radius and the location of the source from which the subsequent position of the element can be determined by integrating the trivial relationship

$$\frac{d\overline{R}}{dt} = \overline{V} \quad \cdots\cdots (16)$$

where $\overline{R}$ is the radius vector of the particle. Therefore, the new radius vector of particle is given by

$$R_{l+dt} = R_1 + \overline{V}dt \quad \cdots\cdots (17)$$

Initial conditions require the efflux velocity, the effluent temperature and salinity. Auxiliary equations including linear interpolations which determine ambient conditions at the level of the particle are also required.

Using the plume element mass ($m = \rho\pi b^2 h$) in terms of its dimensions and density, the plume element radius can be derived as

$$b_{l+dt} = \sqrt{\frac{m_{l+dt}}{\pi\rho_{l+dt}\ h_{l+dt}}} \quad \cdots\cdots (18)$$

The computational procedure in UM model is: 1) a time step is entered, 2) the entrainment equations are solved to calculate the mass amount added in the time step, 3) the increase of the added mass is compared with the target mass increase, and the proper adjustments are made to the time step and the entrainment components to meet the suitable doubling criterion, 4) the motion and other equations are solved, and 5) the new time step is obtained, and the cycle is repeated.

The main approach to solve plume merging is: 1) to reduce the Taylor and forced entrainment areas to consider the loss of exposed surface area when plumes interfere with each other, and 2) to confine each plume mass to the port spacing which is assumed to be symmetric in form. It is assumed that the plumes are identical, and gains equal losses of exposed surface area.

Thus, the Taylor entrainment area is multiplied by a factor which is the ratio of the exposed circumference to the total circumference for the actual exposed area. The suitable ratio of correction is given by

$$a_T = \frac{\pi - 2\phi}{\pi} \quad \cdots\cdots (19)$$

where $\phi = \arctan\sqrt{\frac{4b^2 - L^2}{L^2}}$, on the horizontal plane, the half angle between the line from the center of the plume element to one of the two merged points on the reflection plane and the other line from the center to the other merged point, and L is the adjacent port spacing ($L_r = L\sin\theta$, where L_r is the reduced port spacing, and θ is the angle between current direction and diffuser axis).

The correction factor for the curvature projected area can be expressed as

$$a_{cur} = 1 - \frac{2\phi}{\pi} + \frac{\sin 2\phi}{\pi} \quad \cdots\cdots (20)$$

Now, the distance between the center of the plume element and the merged point on the vertical plane normal to the reflection plane can be solved to give

$$b = \frac{\pi b_r}{\pi - 2\phi + 2\sin\phi\cos\phi} \quad \cdots\cdots (21)$$

where b_r is the unmerged element radius.

In the UM model, the 3/2 power profile (Kannberg and Davis, 1976) is used to calculate the centerline concentration as a function of the average concentration, or dilution, since the profile can match the Gaussian profile over the concentrated portion. The 3/2 power profile is described by

$$\phi = \left[1 - \left(\frac{r}{b}\right)^{3/2}\right]^2 \quad \cdots\cdots (22)$$

where ϕ is the instantaneous scaling factor associated with the differences between the plume properties and the ambient properties and r is the distance between the center of the plume and the point where ϕ is measured.

Using flux integrals for average and centerline concentrations, the peak-to-mean ratio, C_{max}/C_{avg}, can be expressed by integrals:

$$\frac{C_{max}}{C_{avg}} = \frac{C_{max}\int_A dA}{\int_A C dA} \quad \cdots\cdots (23)$$

where the velocity in the plume elements is omitted because it is assumed to be constant.

The RSB model theory is introduced through the projected area entrainment hypothesis (PAE). For unstratified conditions, the dilution, buoyancy frequency, and rise height of the plume can be defined as

$$\frac{S_m qN}{b^{2/3}} = 1.08F^{1/6}$$

$$N = -\left(\frac{g}{\rho_a}\frac{d\rho}{dz}\right)^{0.5} \quad \cdots\cdots (24)$$

$$\frac{z_e}{l_b} = 1.86F^{-1/6}$$

Combining the term, q=Q/L, where L is the diffuser length and Q is the diffuser total volume flux, the minimum initial dilution can be solved to give

$$S_m = \frac{1.08}{1.86}\frac{Lz_e u}{Q} \quad \cdots\cdots (25)$$

where $Lz_e u$ is the flux through the projected area.

However, the peak-to-mean ration of 1.15 used in RSB model is the lower ratio limit which can increase when the additional terms are not neglected. It should be kept in mind that the Taylor and forced entrainment mechanisms act independently, but are mathematically linear (Baumgartner et al. 1994).

3. Sensitivity Analysis for Density Profiles

3.1 Input Parameters

A sensitivity analysis of the plume rise and initial dilution process at the Sand Island Outfall has been performed to identify the degree of influence of effluent flow rate, number of ports, port spacing, port depth, effluent salinity, port diameter, current direction, current speed, and density profile on the plume rise and minimum initial dilution. Conservative values of each parameter were taken from the manual, "Dilution Models for Effluent Discharges" and inputted in both the RSB and UM models as shown in Figure 3 (Baumgartner et al., 1994).

This study focuses on the sensitivity of density profile only since the density stratification is the most important parameter for the submergence of the plume. The RSB and UM models were run to compare the sensitivity of density profiles. The conservative values of the parameters were inputted in both the RSB and the UM model.

The densities obtained from the CTD data are entered without salinity and temperature since the equation for density derivation in the

PLUMES model does not include the pressure effect. The method used for the calculation of density in the CTD data obtained from the City and County is described in the following section.

When densities are entered as input without salinity and temperature, the linear equation of state is invoked since the complex nonlinear equation of state in PLUMES is neglected in

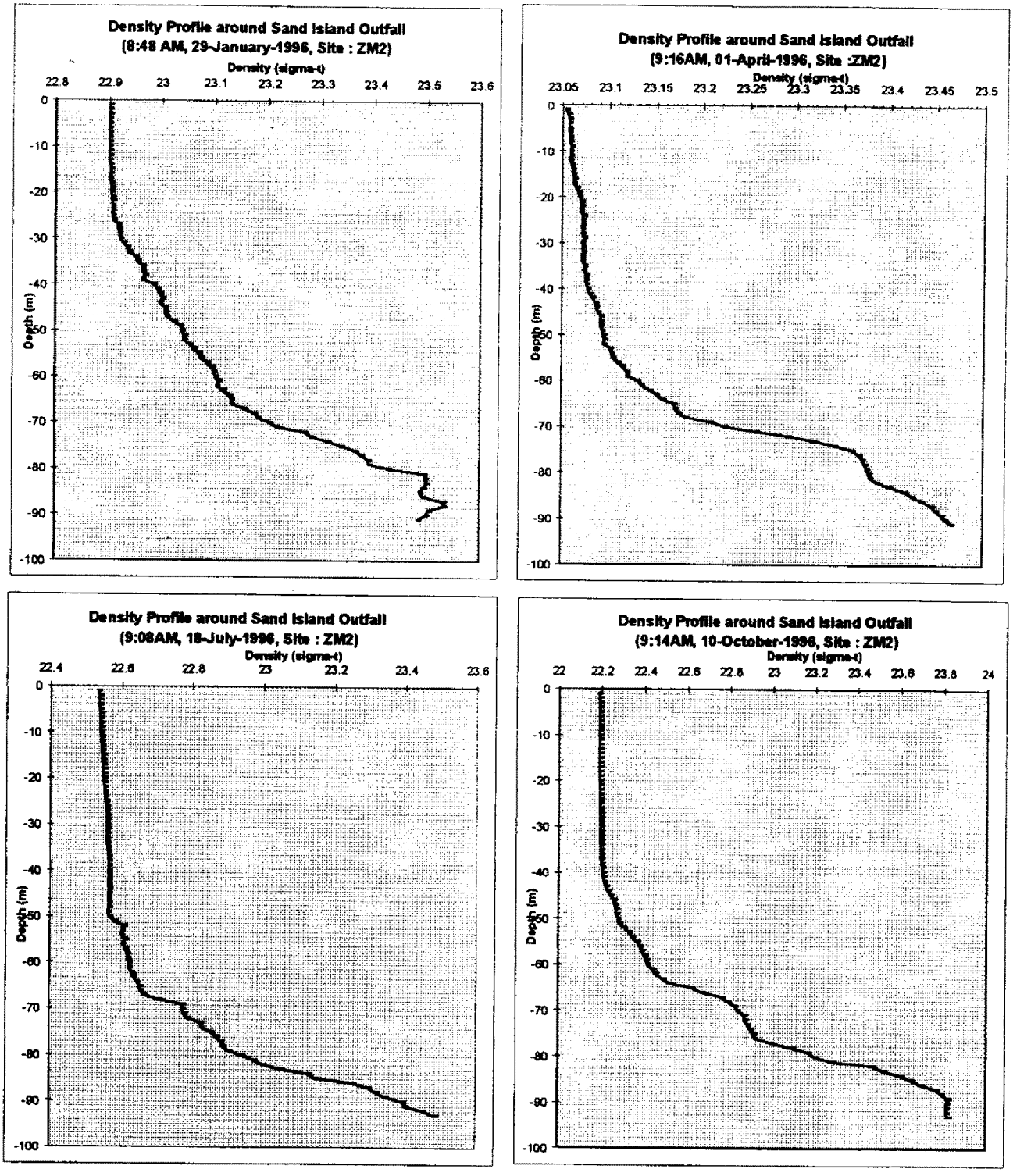

Fig. 2 Density Profiles measured around Sand Island Outfall during 4 different Seasons

```
Apr 10, 1997, 16:48:35 ERL-N PROGRAM PLUMES, Ed 3, 3/11/94 Case:  10 of  11
 Title  Sand Island validation                                  linear
tot flow  # ports  port flow  spacing  effl sal  effl temp  far inc   far dis
 4.469       285   0.015681   3.6575       4.4       25.0      500      2000
port dep  port dia  plume dia total vel  horiz vel  vertl vel  asp coeff  print frq
 70.1     0.085    0.08500    2.763      2.763      0.000      0.10       500
port elev  ver angle  cont coef  effl den  poll conc  decay  Froude #  Roberts F
 0.84       0.0        1.0      0.417376   6.1e8     55.26   20.05      1.044
hor angle  red space  p amb den  p current  far dif  far vel  K:vel/cur  Stratif #
 90         3.657      23.2144    0.1000     0.0003   0.15     27.63      0.00001667
depth  current  density  salinity  temp  amb conc      N (freq)      red grav.
 1      0.1      22.901             0                  0.006546      0.2235
 26     0.1      22.9085            0                  buoy flux     puff-ther
 66     0.1      23.133             0                  0.0009581     1.750
 79     0.1      23.391             0                  jet-plume     jet-cross
                                                       1.604         2.082
                                                       plu-cross     jet-strat
                                                       3.504         5.639
                                                       plu-strat
                                                       10.57
                                                       hor dis>=
```

```
CORMIX1 flow category algorithm is turned off.
 285  L  1040 m                                                1 to any  range
Help: F1.  Quit: <esc>.  Configuration:ATNO1.  FILE: Sandis.var;

                                  RSB

 Case: 10: Sand Island validation

 Lengthscale ratios are: s/lb =  0.63 lm/lb =   0.11
 Froude number, u3/b =          1.06
 Jet Froude number, Fj =        20.3

 Rise height to top of wastefield, ze =      32.6 m
 Wastefield submergence below surface =  37.5 m
 Wastefield thickness, he =          29.0 m
 Height to level of cmax, zm =       21.8 m
 Length of initial mixing region, xi =  101.0 m

 Minimum dilution,        Sm =   447.8
 Flux-average dilution, Sfa =    515.0 ( 1.15 x Sm)
 Wastefield width:    1038.81m   Avg. flux dilution (width*he*u/Q):      674.2
```

```
CORMIX1 flow category algorithm is turned off.
 285  L  1040 m                                                1 to any  range
Help: F1.  Quit: <esc>.  Configuration:ATNO1.  FILE: Sandis.var;
UM INITIAL DILUTION CALCULATION (linear mode)
 plume dep   plume dia   poll conc    dilution    hor dis
    m           m                                   m
     70.10    0.08500     610000000    1.000       0.000
     68.87    1.725        18880000    31.31       4.699
     66.59    3.674         5760000    101.0       8.316 -> merging
     56.23    20.64          944700    551.7       27.07 -> trap level
     51.51    36.55          514300    883.8       49.20
 -> local maximum rise or fall
```

Fig. 3 PLUMES RSB and UM runs for the Sand Island Outfall

favor of the simple linear equation of state. However, the linear form of the model results in slight errors in the predictions except when a plume is discharged into very cold and fresh water which can lead to significant errors (Baumgartner et al., 1994). Therefore, the slight error in this prediction can be neglected since the ambient water is relatively warm and saline.

3.2 Sensitivity of Density Profile

The variations of the wastefield behavior are not significantly sensitive within the range of effluent flow rate, number of ports, port depth, effluent salinity, and port diameter. Fig. 4 describes sensitivity analysis for different density profiles using the RSB and UM models. The density profiles used here were from CTD measurements at ZM2 on January 29, April 1, July 18, and October 10, 1996 as shown in Figure 2. In the density profiles measured during January, April, and July, the weakly stratified density distributions are shown over the lower portion of the column above the depth of 70.1m. This effect may result in higher plume rise while the somewhat strong density stratification from the density profile measured during October likely leads to a deeply submerged wastefield as shown in Fig. 4. It is proved that the plume rise and minimum dilution are significantly sensitive to the density profiles. In other words, the increments close to a linear distribution from nonlinear density profiles measured over whole depth should be linearized as much as possible, especially on stratification, for a more reliable description of wastefield behavior.

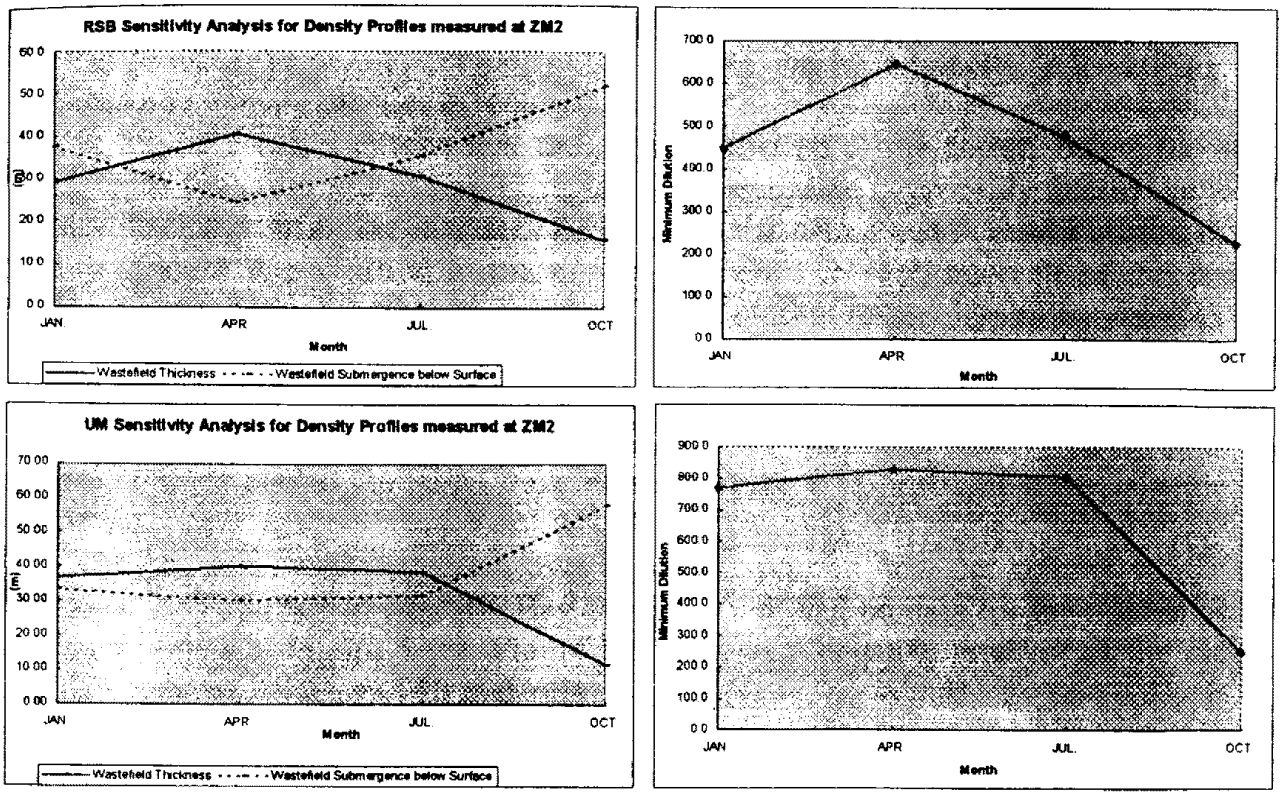

Fig. 4 Sensitivity Analysis for the Different Density Profiles using the RSB and UM models

4. Density Profile

4.1 Measurement of the Density Profile

As discussed above, the density stratification over the water column has significant impacts on the plume behavior such as rise height and dilution. The density profiles can be obtained from the salinity and temperature profiles which are basic and important characteristics of sea water. The salinity and temperature over entire depth are measured using instruments that measure temperature using a thermocouple and convert the conductivity measurement into salinity and temperature where the principle of the conversion is based on the Wheatstone Bridge.

Using the measured depth, temperature, and salinity, water density can be calculated by the following relationship:

$$\rho(S, t, p) = \rho(S, t, 0)/[1 - p/K(S, t, p)] \quad \cdots (26)$$

where S is the salinity (‰), t is the temperature (℃), p is the sea pressure (bars), K is the bulk modulus ($=1/\beta$), and β is the compressibility of sea water (Pickard, 1990). In this equation, the influence of pressure is described using a high pressure version to provide the bulk modulus. Millero et al.(1980) derived the polynomial expressions for this relationship.

4.2 Linearization of the Density profile

There are several types of the density profiles measured by City & County. Among them, somewhat jagged and negative gradient of the density profiles are present. Fig. 5 shows several examples of the density profiles measured around the Honouliuli outfall. In order to input the density profiles in the PLUME model, a reasonable linearization of the measured density profiles is required.

In Fig. 5-(a), it is seen that the jagged variation of the density below the 40 m depth tends toward a lower density region. This variation is probably due to the lower density discharge from the diffuser. To linearize the background density profile in this case, a straight line is fitted to the maximum values in each intervals of the density profile. On the other hand, in Fig. 5-(b), the variation of the density between 45 and 55 m depth tends to be zigzag around the general profile trend, which may be due to eddy circulation of the deep water. Hence, the straight line is fitted to the mean values in each intervals of this density profile. In Fig. 5-(c), the large density variation at the surface is likely due to the initial inequilibrium of the CTD instrument and is neglected in this analysis.

The positive density gradient over the upper portion of water column which was not taken into account in Mamala Bay Study (which had no data for the uppermost 15 m) is presented in Fig. 5-(d). Fig. 5-(e) shows a negative gradient of the density profile between surface and 50 m depth.

4.3 Influence of the Density Gradient over the Upper Portion of Water Column

In the Mamala Bay Study, the positive density gradient over the upper portion of water column has not been taken into account due to the fact that the 11 thermistors at 5 m depth increments were deployed only from 15 to 65 m depth at the Honouliuli outfall (Roberts 1995). Fig. 5-(c) and (d) show typical examples of the positive density gradient over this upper portion. Parts, (a) and (b), in Table 1 are the plume behavior

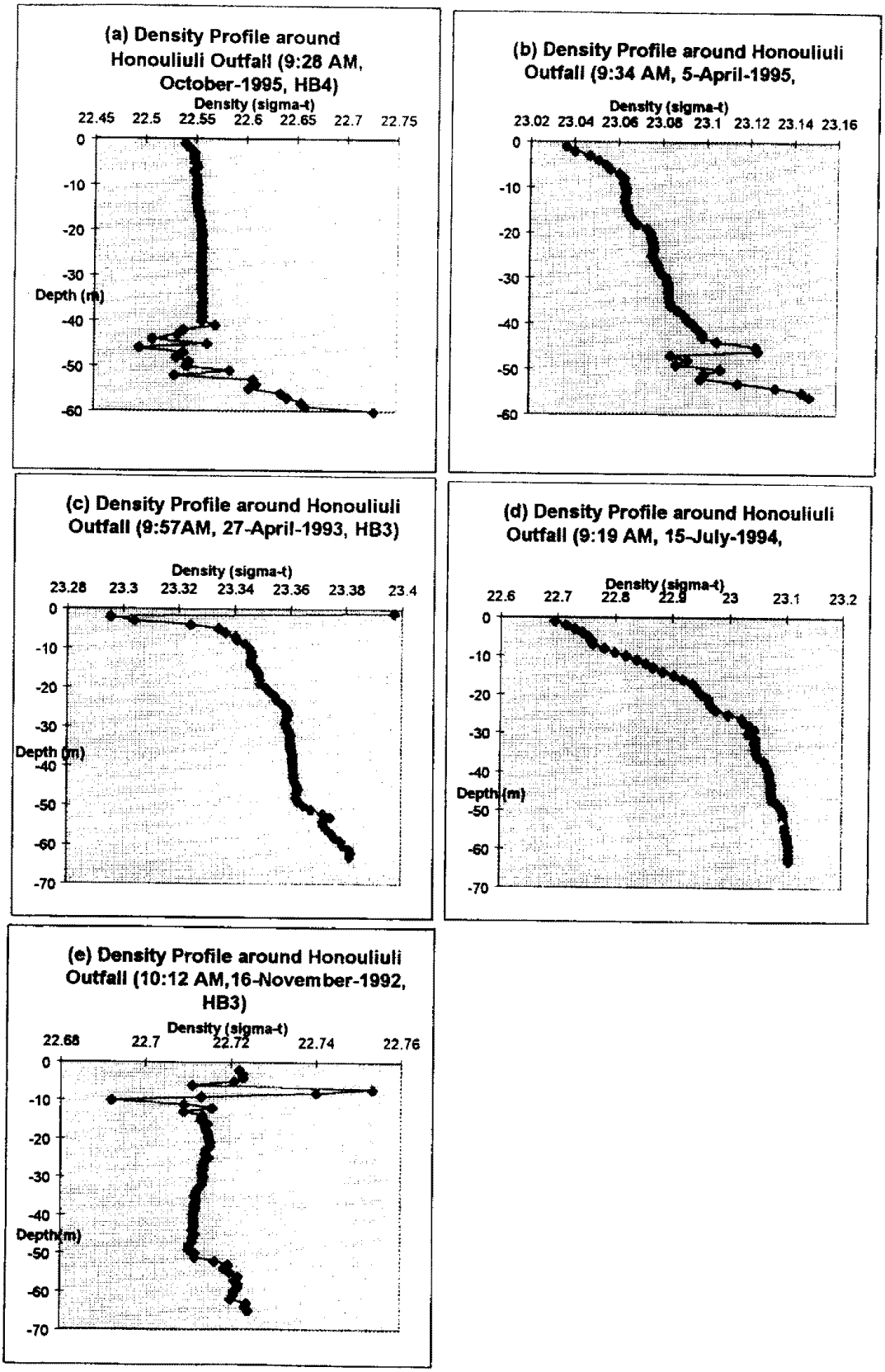

Fig. 5 Density Profiles measured around the Honouliuli Outfalls

Table 1 The Comparison between the Plume Behavior predicted by the Different Increments of Density Profiles

(Definition of Variables)

he : Wastefield Thickness
hz : Wastefield Submergence below Surface
zm : Height to Level of Maximum Concentration
Sfa : Flux-Average Dilution
hm : Level of Maximum Concentration below Surface

	(RSB RUN)					(UM RUN)					
	Stations	he (m)	hz (m)	zm (m)	Sfa	he (m)	hm (m)	hz (m)	zm (m)	Sfa	
(a)	HB3 (t=0)	49.3	7.3	38.8	2546.9	61.25	29.91	0.00	32.09	2146.0	>> Surface Hit
	HB3 (t=2)	49.8	5.8	41.6	2300.4	60.46	28.84	0.00	33.16	1826.0	>> Surface Hit
	HB3 (t=4)	48.6	3.7	45.5	1605.1	41.29	12.24	0.00	49.76	366.4	>> Surface Hit
	HB3 (t=6)	51.0	3.1	39.5	1240.6	41.06	12.07	0.00	49.93	1044.0	>> Surface Hit
	HB3 (t=8)	52.4	3.1	39.5	1236.7	44.12	14.68	0.00	47.32	1560.0	>> Surface Hit
(b)	HB3 (t=0)	54.6	0.0	43.0	2821.6	>> Surface Hit	61.18	29.84	0.00	32.16	2146.0	>> Surface Hit
	HB3 (t=2)	53.6	0.0	44.8	2476.2	>> Surface Hit	60.37	28.76	0.00	33.24	1826.0	>> Surface Hit
	HB3 (t=4)	50.6	0.0	47.3	1666.7	>> Surface Hit	41.14	12.17	0.00	49.83	366.4	>> Surface Hit
	HB3 (t=6)	47.7	0.0	45.3	1293.6	>> Surface Hit	40.60	11.88	0.00	50.14	1044.0	>> Surface Hit
	HB3 (t=8)	47.7	0.0	45.3	1289.5	>> Surface Hit	43.35	14.26	0.00	47.74	1560.0	>> Surface Hit
(c)	HB3 (t=0)	31.7	25.7	24.4	1451.2		54.38	35.64	8.45	26.36	1763.0	
	HB3 (t=2)	31.7	25.3	24.6	1274.1		59.91	33.11	3.16	28.89	1464.0	
	HB3 (t=4)	31.5	23.9	25.5	884.7		50.43	16.93	0.00	43.07	339.6	>> Surface Hit
	HB3 (t=6)	33.5	23.3	25.9	738.6		47.99	28.16	2.19	35.82	853.8	
	HB3 (t=8)	34.4	23.3	25.9	734.7		40.00	31.50	11.50	30.50	1088.0	
(d)	HB3 (t=0)	29.8	27.8	22.9	1399.5		53.28	36.07	9.43	25.93	1728.0	
	HB3 (t=2)	30.4	26.8	23.6	1258.3		59.48	33.33	3.59	28.67	1453.0	
	HB3 (t=4)	31.3	24.2	25.3	923.1		50.42	16.90	0.00	43.10	339.6	>> Surface Hit
	HB3 (t=6)	33.8	22.9	26.2	741.3		42.05	27.56	6.56	34.42	785.6	
	HB3 (t=8)	34.8	22.9	26.2	737.4		40.56	31.46	11.18	30.54	1098.0	

Note : (a) Plume behavior calculated with a linearized density profile in 1 m depth increments (from Fig. 5-(c))

(b) Plume behavior calculated by using the increments used in Mamala Bay Study (from Fig. 5-(c))

(c) Plume behavior calculated with a linearized density profile in 1 m depth increments (from Fig. 5-(d))

(d) Plume behavior calculated by using the increments used in Mamala Bay Study (from Fig. 5-(d))

determined by the density profile (Fig. 5-(c)) while the parts, (c) and (d), are the plume behavior determined by the density profile (Fig. 5-(d)). In order to identify the plume behavior generated by the positive density gradient in upper part, the plume behavior ((a) and (c)) obtained with a linearized density profile in 1 m depth increments and the plume behavior ((b) and (d)) obtained by using the increments used in Mamala Bay Study are compared in Table 1. In (a) and (b), the plume behavior predicted by the UM model shows good agreement whereas the plume behavior calculated by the RSB model shows relatively poor agreement as presented in Fig. 6. In addition, in Table 1-(b), all the plumes predicted by the RSB model without considering the upper density gradient reach the surface while, in Table 1-(a),

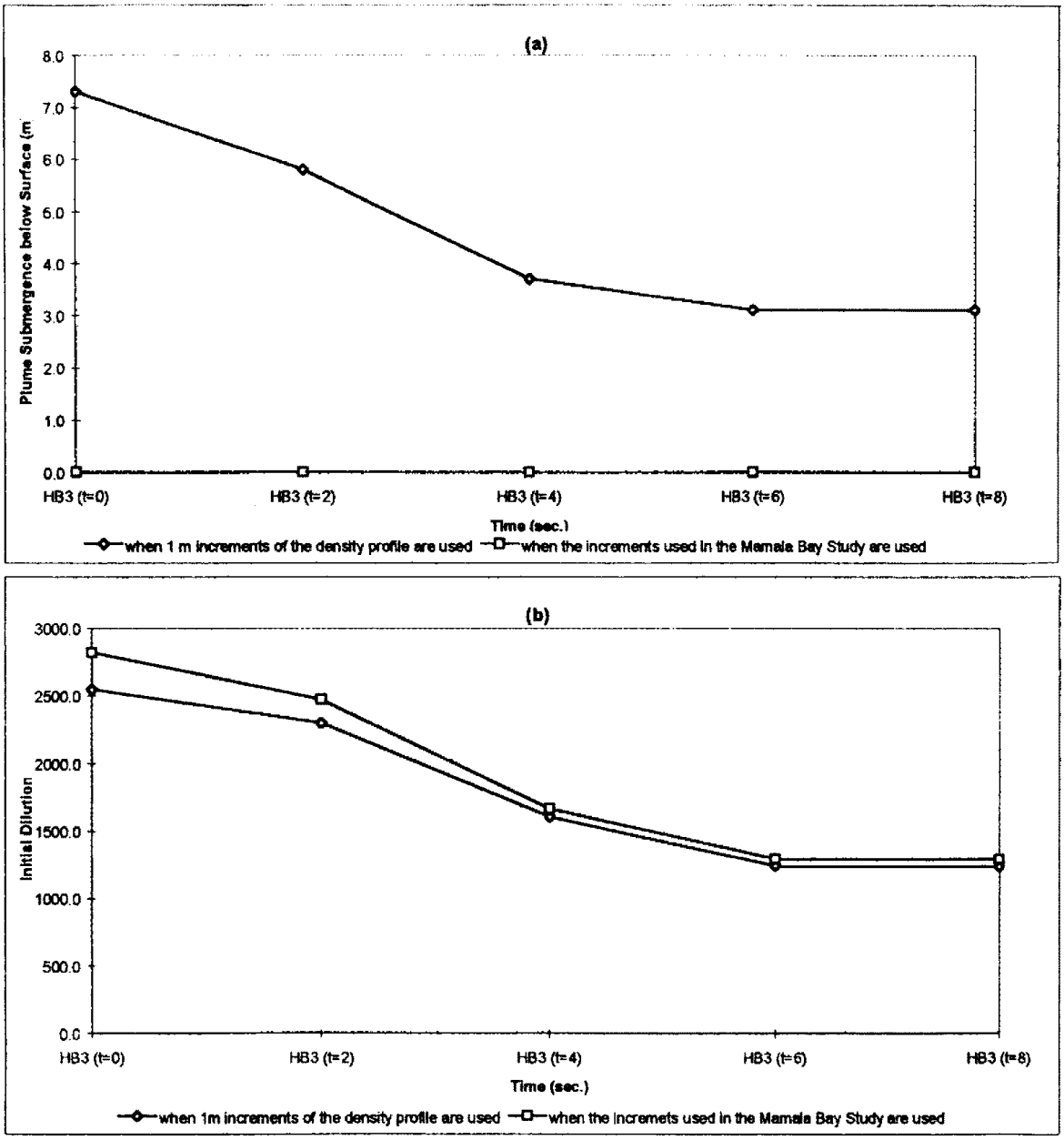

Fig. 6 Comparison between the Plume Rise and Initial Dilution (calculated by the RSB model) predicted by the different Increments of Density Profiles in case of the Plume shallowly Submerged (by Table 1-(a) and (b))

the plumes predicted by the RSB model including the upper portion are shallowly submerged. In (c) and (d), the plume behavior predicted by both the RSB and UM models shows good agreement since the calculated plume is submerged in the middle region of water column. It is noted that the plume rise and initial dilution calculated by the UM model are in good agreement between the density profiles measured by the different increments regardless of the degree of the plume rise. In Fig. 6-(a) and (b), it is noted that the positive density gradient

over the upper part results in lower plume rise and initial dilution in the case of shallowly submerged plume. It is seen that, in the RSB model, the density profile over the entire water column should be taken into account for more reliable description of plume behavior.

5. Conclusion

The plume rise and initial dilution calculated by the RSB and UM models are significantly sensitive to the density profile. The weakly stratified density distributions over the lower portion of the column result in higher plume rise while the somewhat strong density stratification leads to a deeply submerged wastefield. The UM and RSB models are reliable and recent models used herein for the prediction of wastefield behavior at both outfalls since both models support each other, but are certainly identical.

The positive density gradient over the upper portion of water column as a common characteristic in the real world has been taken into account in this study. In the plume behavior calculated by the RSB model, it is observed that the positive density gradient over the upper part leads to lower plume rise and initial dilution in the case of shallowly submerged plume. It was mentioned that the Mamala Bay Study used the RSB model for the calculation of the plume rise and initial dilution. In other words, it is expected that the surfacing frequency (calculated by the RSB model) reflecting the positive density gradient over upper portion is definitely lower than the surfacing frequency predicted in the Mamala Bay Study which did not take into account the density distribution in upper part. Therefore, it is strongly suggested that following studies should take into account the density profile over entire water column for more reliable plume behavior description.

요 약

미국에서는 오래 전부터 보다 효율적인 폐수 처리를 위해 1차 처리된 폐수를 연안의 폐수처리장으로부터 긴 관을 통해 심해저로 흘러 보내고 있고 큰 효과를 보는 것으로 알려져 있다. 그러나, 심해저 확산배출구를 통해 흘러 나와 형성된 플룸이 근접한 연안에 간접적으로는 인간의 건강에 해를 줄 수가 있기 때문에 바다의 물리적인 조건과 지형적인 조건을 고려한 심해저 확산배출구의 적절한 수심에서의 배치가 필수적이라 하겠다.

미국의 세계적인 관광 도시 호놀룰루시가 위치해 있는 오하우섬 남쪽에서는 위치의 중요성과 다량의 배출 폐수 때문에 중요시되는 샌드 아일랜드 배출구와 호노울리우리 배출구가 관심의 대상이 되었으며 현재까지 확산배출구의 배치에 적합한 수심선정에 대한 타당성 연구가 진행되어져 왔다. 최근에는 9백만 불의 지원을 받아 행한 마말라 만에 대한 이전의 연구(프로젝트MB-4)에서는 샌드 아일랜드의 확산 배출구 주위에서 플룸의 표면수 도달 빈도가 실질적인 값보다 훨씬 높은 값으로 계산되었는데 본 논문에서는 마말라 만에 대한 연구의 단점을 보완하고 마말라 만 연구에서와 같은 모델을 이용하여 플룸의 표면수 도달 빈도와 초기 희석도를 실질적인 값에 거의 근접시키는데 성공했다.

본 논문에서 중요시한 것은 마말라 만 연구에서 선택된 특정 모델의 입력 변수 중에서 배출구 주위의 해수 컬럼에서 상층과 전체적인 밀도분포를 고려하지 않은 데서 오는 단점을 보완하여 1미터 간격으로 측정된 상층을 포함한 현실적인 밀도분포를 이용하고 플룸의 상승과 초기 희석도를 계산할 때 상층의 밀도 분포를 고려하였다. 앞으로의 연구에서 상층과 전체적인 밀도 분포를 고려함으로써 예측 수치를 더욱 현실 값에 접근시킬 수 있음을 입증하였다.

References

1) Baumgartner, D.J., Frick, W.E., and Roberts, P.J.W. (1994). "Dilution Models for Effluent Discharges (Third Edition)." U.S. Environmental Protection Agency, Office of Research and Development, Washington, DC. EPA/600/R-94/086.

2) De Jesus T.M.C. (1984). "Current and Mixing Measurement Techniques for the Sand Island Ocean Outfall." Department of Ocean Engineering, University of Hawaii.

3) Krock, H.J. (1996). "Review of the Mamala Bay Study" Mamala Bay Study, Mamala Bay Study Commission, Appendix II, Appendix B.

4) Muellenhoff, W.P., Soldate, A.M., Baumgartner, D.J., Schuldt, M.D., Davis, L.R., and Frick, W.E. (1985). "Initial Mixing Characteristics of Municipal Ocean Discharges." U.S. Environmental Protection Agency, Report no, EPA-600/3-85-073a.

5) Pickard, G.L. and Emery, W.J., (1990): Descriptive Physical Oceanography (An Introduction). Pergamon Press, Oxford etc.

6) Roberts, P.J.W. (1995). "Plume Modeling." Mamala Bay Study, Mamala Bay Study Commission, Volume 1, Report No. Project MB-4.

7) Roberts, P.J.W., Snyder, W.H., and Baumgartner, D.J. (1989a). "Ocean Outfalls. I: Submerged Wastefield Formation. "Journal of Hydraulic Engineering, ASCE, 115(1), 1-25.

8) Roberts, P.J.W., Snyder, W.H., and Baumgartner, D.J. (1989b). "Ocean Outfalls. II: Spatial Evolution of Submerged Wastefield." Journal of Hydraulic Engineering, ASCE, 115(1), 26-48.

9) Roberts, P.J.W., Snyder, W.H., and Baumgartner, D.J. (1989c). "Ocean Outfalls. III: Effect of Diffuser Design on Submerged Wastefield." Journal of Hydraulic Engineering, ASCE 115(1), 49-70.